INSTITUTE OF PHYSICS PUBLISHING JOURNAL OF PHYSICS B: ATOMIC, MOLECULAR AND OPTICAL PHYSICS

J. Phys. B: At. Mol. Opt. Phys. **36** (2003) 3043–3054 PII: S0953-4075(03)59756-5

Experimental study of K-shell ionization of low-Z solids in collisions with intermediate-velocity carbon ions and the local plasma approximation

U Kadhane[1], C C Montanari[1,2] and Lokesh C Tribedi[1]

[1] Tata Institute of Fundamental Research, Homi Bhabha Road, Colaba, Mumbai 400 005, India
[2] Instituto de Astronomía y Físca del Espacio, CONICET-UBA, Buenos Aires, Argentina

E-mail: lokesh@tifr.res.in

Received 18 February 2003, in final form 15 May 2003
Published 4 July 2003
Online at stacks.iop.org/JPhysB/36/3043

Abstract

K-shell vacancy production in low-atomic-number ($Z_t = 17$–29) solid targets has been measured in collisions of highly charged carbon ions with energies of 1.5–6 MeV u^{-1}. The K-shell ionization cross sections of Cl, K, Ti, Fe and Cu are derived from the measured K x-ray cross sections. The present data-set has been used to test the predictions of a theoretical model based on the local plasma approximation (LPA). This theory takes into account the response of solid core electrons working within the dielectric formalism. We find that this *ab initio* ion–solid model gives very good agreement with the measured data for Fe and Cu targets, while it tends to under-estimate the data for the most symmetric collision systems studied here. We discuss the range of validity of the LPA in terms of the symmetry parameter and the impact velocity. On the other hand, a model based on the perturbed stationary state approximation, designed for ion–atom collisions (ECPSSR) is found to give excellent agreement with the measured data for all target elements over the whole energy range. All the measured cross sections for different targets are found to follow a universal scaling rule predicted by the ECPSSR.

1. Introduction

Studies on ionization of atoms by impact of charged particles provide a valuable insight into the dynamics of ionic collisions with molecules, clusters, solids and surfaces in general. In the case of highly charged heavy projectiles, the collision dynamics become more complicated since the initial as well as the final states of target electrons are strongly distorted by the projectile charge. The two-centre effect [1] is known to influence the ionization mechanisms, even for simple collision systems involving multiply charged bare ions impinging on atomic H or He targets at high velocities [2–6]. Since the pioneering work of Bates and Griffing in the 1950s [7], there has been a lot of progress in the understanding of ion–atom ionization

mechanisms. The *ab initio* continuum distorted wave calculations (CDW and CDW-EIS, where EIS stands for eikonal initial state) [8] have been quite successful in describing two-centre electron emission in the ionization of atomic hydrogen or helium (for which the electrons are loosely bound) [2, 4, 9, 10]. However, in the case of ionization of strongly bound electrons belonging to multi-electron targets (i.e. K ionization of Ar and Kr by heavy ions) CDW-EIS fails to reproduce the total ionization cross sections [11, 12].

There are many studies on the total ionization of deeply bound electrons, and several empirical scaling laws have been proposed [13, 14]. Some of the experimental results on the inner-shell ionization can be found in various compilations [14–18] and in other references [11, 12, 19–23].

Most of the theories, however, have been developed for collisions in which the target is a single gas atom or molecule. Some of the commonly used models are not *ab initio* models but are semi-empirical in nature. However, they are quite successful in reproducing many experimental data for relatively complicated atoms, for which an exact and *ab initio* calculation is extremely difficult. An example of this is the well known ECPSSR approximation [13]. This model is based on the perturbed stationary state (PSS) approximation, with modifications introduced in the B1 approximation to account for the effects due to the polarization and enhanced binding energy of the target electrons, Coulomb (C) deflection, energy loss (E) and relativistic (R) wavefunctions in a semi-empirical manner. The successful description of experimental data via an analytical expression makes the ECPSSR approximation very convenient in evaluating K-shell ionization cross sections, although it is not an *ab initio* calculation.

Additional complications arise if the collision system involves a solid target. In such collision systems the solid-state effect, which arises from the large electron density fluctuation and plasmon excitation, is known to influence the atomic collision processes, as evident from many experimental results in the past [24–31]. Most of the studies on atomic collisions with solids are related to the interaction of the ion with the free electron gas (FEG). However, high-velocity experiments have shown that the target inner-shell electrons also contribute to the dynamic screening and therefore these electrons should be considered in order to have a complete picture of the dynamic screening of the ion [30, 32, 33]. One of the models for dealing with core-electron polarization is the local plasma approximation (LPA). Details of the LPA calculations can be found in [33, 34] and references therein (see below).

The present work is an attempt to test the validity of the LPA in the intermediate-velocity range. The aim of this work is then to present new measurements of K-vacancy production inside solids and to compare the data with two different theoretical approaches. On one side, the ECPSSR, which belongs to binary collisional formalism, is used extensively in inner-shell ionization, but it is not an *ab initio* theory. On the other side, the LPA is an *ab initio* model that works within the dielectric formalism, introducing a collective description of the solid electrons. A link between the binary collisional formalism and the dielectric formalism has been developed by Miraglia and co-workers [31, 35], showing the relation between both descriptions.

2. LPA model and the range of its validity

The dielectric formalism, which is generally employed to deal with the FEG in describing the interaction with the solid, has been extended to account for the inner-shell process by using the LPA. In summary, this model assumes that:

(i) the bound electrons react to the external perturbation as free particles, which can be described at each point of space $\vec{r}$ as belonging to a FEG with a local Fermi velocity $k_{\mathrm{F}}(r) = [3\pi^2 n(r)]^{1/3}$, where $n(r)$ is the electronic density;

(ii) the corresponding dielectric function for the bound electrons is a spatial mean value of the Lindhard dielectric function, $\varepsilon(q, \omega, n(r))$ [36].

Though the LPA has been formulated to describe the core-electron response as a whole, the present version allows us to consider the excitation of each shell separately (for instance, to evaluate the K-shell ionization cross sections). The model describes the inner-shell electrons as a FEG of inhomogeneous density. This approximation is expected to be valid for bound electrons with orbital speeds smaller than the ion velocity ($v_p \geqslant v_e$). This high-velocity model considers the action of the effective potential that is produced by the external charge, Z_p, to the first order of perturbation. Good agreement with the experimental data is found, even for projectile velocities lower than this value [34]. The LPA calculations have been found to reproduce the K-shell ionization cross sections extremely well for highly asymmetric collision systems, such as Al, Si and Cu, by proton impact for velocities between 2 and 20 au [34]. On the other hand, the model deviates substantially from the measured K-ionization cross sections for more symmetric collision systems, such as highly charged oxygen ions colliding on Cl, K and Ti in the intermediate-velocity range [37]. Since the applicability of the theoretical model depends on the symmetry parameter (and hence the perturbation strength) of the collision ($S_Z = Z_p/Z_t$) we have now used highly charged carbon ions colliding on a set of low-Z_t targets in order to have a variation of S_Z over a wide range (between 0.21 and 0.35). This, combined with the low-to-intermediate velocity range ($v_p/v_e \leqslant 1.0$), provides the collision systems which are highly non-perturbative for some of the targets used. These data, along with the proton- and oxygen-induced K-ionization data, will help in exploring the applicability of the model over a wide range of symmetry parameters and over a range of generalized perturbation strengths (see below).

There have been many applications of this model, from the original proposal of Lindhard and co-workers [38] to more recent calculations of the coupling of projectile orbitals by the induced potential [33] or the contribution of deep bound electrons to the stopping power and energy straggling [34, 39], all providing results in good agreement with experimental measurements.

3. Experimental details and data analysis

A well collimated beam of carbon ions with energies between 24 and 85 MeV was provided by the BARC–TIFR Pelletron facility at TIFR. The energy and charge state analysed ion beam was made to pass through a post-acceleration foil stripper to obtain higher charge states, and a switching magnet was used to select a particular charge state. The charge states of the projectiles were 4^+, 5^+ and 6^+. Targets of K, Cl (in the form of KCl), Ti, Fe and Cu were prepared on 10 μg cm^{-2}-thick C backing with thicknesses of 1.6, 1.6, 2.43, 0.58 and 1.9 μg cm^{-2}, respectively. Such thin targets were chosen to ensure single-collision conditions. The targets were mounted on a rotatable multiple target holder assembly. The K x-rays, which arise due to the production of the target K-shell vacancy and its decay, were detected using a Si(Li) detector of 30 mm^2 in area and 3 mm in thickness mounted inside the vacuum at an angle of 45° with respect to the beam direction. The detector was equipped with a Be window of thickness 25 μ and a resolution of 165 eV at 6.9 keV. A silicon surface barrier detector was mounted at 135° to detect the elastically scattered particles. This was used to measure the target thickness *in situ* at lower energies than the Coulomb barrier for all target–projectile combinations. The target chamber was electrically isolated from the beam line and the vacuum pump in order to collect the charge on the entire chamber, which was used for normalization.

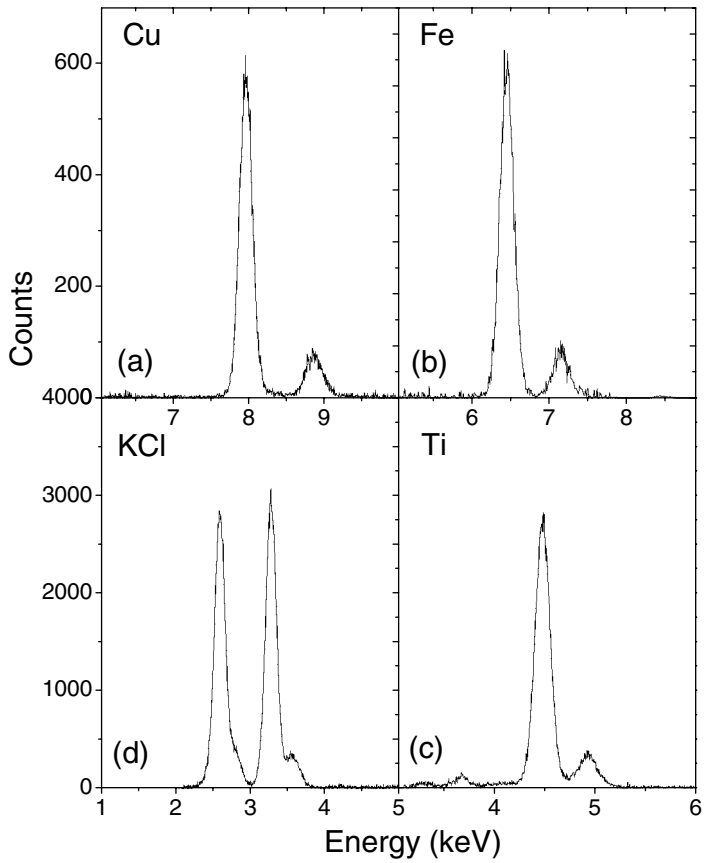

Figure 1. The x-ray spectrum emitted from various targets in collision with 66 MeV C^{5+}.

The data were collected on a CAMAC-based high-speed data acquisition system interfaced to the PC.

Typical x-ray spectra at a beam energy of 66 MeV for each target are presented in figure 1. For the case of Cu, Fe and Ti, the Kα and Kβ lines are well separated; for the case of K and Cl, these lines are not well resolved. The spectra were analysed by using a multi-parameter fitting program to obtain the peak position and intensity. The intensities were corrected for the detector efficiency and transmission through the Be window. The K-ionization cross sections were derived from the measured x-ray cross sections and the K-shell fluorescence yields, ω_K. The ω_K values were taken from the tabulation by Krause [40] and were further corrected for multiple ionization of the outer shells in the target. These corrections were estimated by using the calculated data tables provided by Bhalla [41], the measured intensity ratios of the Kα and Kβ lines, and the shifts in these x-ray energies (see table 1). The enhancements in the values of ω_K were found to be between 9 and 22% (table 1). The vacancy-production cross sections that were derived for lower-charge states (i.e. with no K-shell vacancy, σ^0_{KV}) are found to be almost independent of charge states and are taken as Coulomb ionization cross sections (σ_{KI}). The derived cross sections are shown in table 1. The typical error is about 15–20% for ionization cross sections, which includes the uncertainties in the target thickness, detector solid angles, fluorescence yields, and counting statistics.

Table 1. The ionization cross sections (σ_{KI}), energy shifts (ΔE_α and ΔE_β), intensity ratios, and the enhancements in fluorescence yields.

Target	Energy (MeV)	q^+	ΔE_α (eV)	ΔE_β (eV)	I_β/I_α	$\omega_{\mathrm{K}}/\omega_o$	σ_{KI} (kb)
Cl	30	4	35	66	0.094	1.13	278.7
	40	4	30	50	0.123	1.13	332.6
	50	4	25	25	0.120	1.13	371.4
	66	6	20	30	0.116	1.05	398.2
K	30	4	35	96	0.132	1.13	124
	40	4	30	71	0.137	1.13	185
	48	5	25	60	0.17	1.13	233
	50	4	25	55	0.139	1.13	206
	60	5	25	55	0.183	1.13	220
	66	6	20	45	0.147	1.13	225
	72	5	15	35	0.142	1.05	173
	84	6	15	30	0.195	1.05	207
Ti	30	4	35	96	0.132	1.123	45.62
	40	4	30	79	0.130	1.115	72.8
	50	4	25	55	0.136	1.070	89
	66	5	20	45	0.131	1.070	115
Fe	40	4	35	100	0.142		17
	48	5	30	90	0.152		26.15
	60	5	25	75	0.135		31.81
	72	5	20	60	0.151		41.18
	84	6	20	65	0.131		49.62
Cu	24	4	45	95	0.179	1.11	1.56
	30	4	40	100	0.168	1.11	2.96
	40	4	35	80	0.155	1.11	6.37
	48	5	30	80	0.155	1.11	10.27
	50	4	25	70	0.155	1.11	10.45
	60	5	35	70	0.149	1.11	13.59
	66	5	30	55	0.153	1.11	18.85
	72	5	20	60	0.165	1.05	17.69
	84	6	20	60	0.152	1.05	23.29

4. Results and discussion

4.1. X-ray energy shifts

For the case of the heavy ion–atom interaction, the energies of the Kα and Kβ lines increase from that of a singly ionized atom. This is due to the fact that there are multiple vacancies in the L and M shells simultaneous with the K x-ray emission. The shifts depend on the beam energies as well as the projectile's atomic numbers, since the L-ionization cross sections depend on these parameters. In figure 2 we display the beam-energy dependence of the energy shifts of the Kα and Kβ lines. It may be seen (see the inset, also) that the energy shifts are independent of the beam charge states (different data points at a given energy are for different charge states). This behaviour is different to that for gaseous targets, for which the energy shifts are known to be dependent on the charge states (see, for example, [11, 12]). For the case of solid targets, as in the collision systems being considered, the charge state of the projectile gets equilibrated within a few monolayers of the target. The uncertainties in the peak energies of Kα and Kβ were approximately 10 and 20 eV, respectively. The shifts in the peak energies

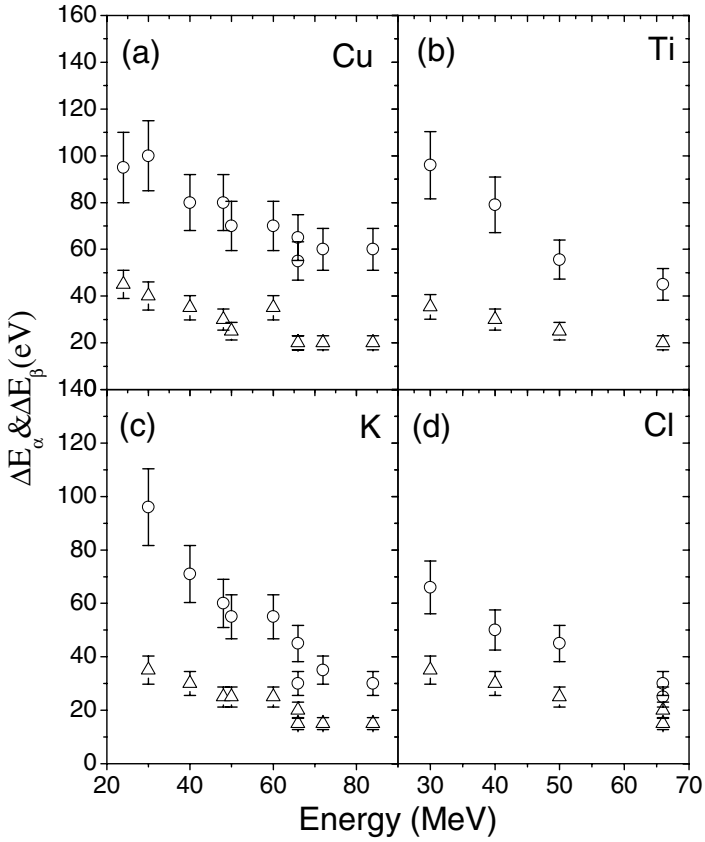

Figure 2. The energy shifts of the Kα and Kβ lines for (a) Cu, (b) Ti, (c) K and (d) Cl targets in collision with carbon ions. The different data points (of the same symbol) at the same energy correspond to different charge states of the projectile.

decrease as a function of beam energy (figure 2). This is expected, however, since the beam velocities (10–17 au) are much higher than the M- and L-shell orbital velocities of the target electrons.

4.2. K-ionization cross sections and comparison with the ECPSSR

Figure 3 shows the comparison of K-shell ionization cross sections with the ECPSSR model. The model (solid curve) shows excellent agreement with the measured data over the whole range of velocities and for all targets. In the case of H-like or bare ion projectiles, the vacancy productions in the target K shells could also be due to K–K electron transfer from the target K shell to the projectile K shell (since K–L transfer is negligibly small). The theoretical calculation shown by the dash–dotted line includes the K–K transfer cross sections (σ_{KK}) based on the PSS model of Lapicki and co-workers [43, 44], along with the ECPSSR predictions. These calculations are shown for the data taken with H-like or bare ions. However, it is worth mentioning that, for the present collision systems, we found that the K–K transfer cross sections are only a small fraction of the K-ionization cross sections. For example, for the case of the most asymmetric collision (i.e. C on Cu), σ_{KK}/σ_{KI} is only about 5–15% over the whole energy range. For the case of the other extreme, i.e. for the most symmetric collision

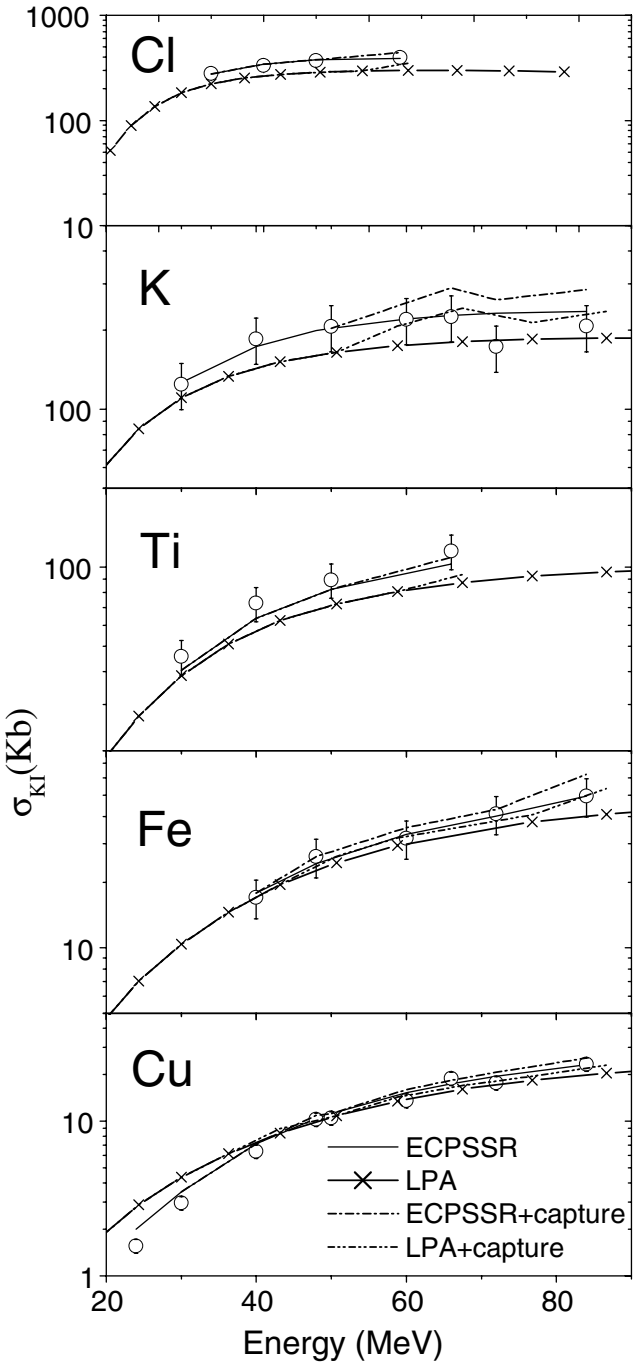

Figure 3. The K-shell ionization cross sections for different targets as a function of beam energy, compared to the LPA and ECPSSR models (crosses joined by solid curves and solid curve, respectively). The charge states of the carbon ions correspond to the zero vacancy in the K shell, except in a few cases (see text and table 1) for which the H-like and bare ions were used. For these charge states, the K–K transfer cross sections were calculated (see text) and added to the LPA (see dash–dot–dot curve) and to the ECPSSR predictions (dash–dot curve).

(C + K or C + Cl), this fraction was found to be 10–20%. At some energies (such as 66 MeV) both the 5^+ and 6^+ charge states were used. In such cases the difference between these two cross sections gave the σ_{KK}, and therefore the K-ionization cross sections could also be determined (since $\sigma_{KI} = \sigma_{KV}^{5+} - \sigma_{KK}$). The ECPSSR—although semi-empirical rather than *ab initio* in nature—reproduces the experimental data for the asymmetric collisions. The good agreement with the experimental data displayed in figure 3 clearly indicates that, for the inner-shell ionization, this ion–atom model is applicable for describing ion–solid collision experiments, using the present collision parameters (provided that sufficiently thin targets are used in the experiment, to ensure the single-collision condition).

4.2.1. Universally scaled cross sections. According to first-order perturbation theory, a properly scaled K-shell ionization cross section can be expressed as a function of the scaled velocity only and independently of the actual target projectile combination. It has been shown in the past that, if the scaled cross sections for K-shell ionization are plotted as a function of the scaled velocity parameter, then the different data-sets fall on a universal PWBA curve [14]. It has also been shown recently [46] that such a scaling rule holds good, approximately, even for K-ionization cross sections for high-Z_T elements for which the relativistic wavefunction effects strongly influence the cross sections. In order to test the validity of these scaling laws, we have plotted, in figures 4(a) and (b), the reduced cross sections as a function of the scaled velocity for the cases of C and O projectiles, respectively. The figure 4(c) shows both data-sets together. The scaled variables and the scaling procedure are defined in the literature [13]. All the data points are found to follow the universal curve predicted by the ECPSSR model.

4.3. Comparison with the LPA

It can be seen in figure 3 that the *ab initio* LPA calculations (crosses joined by a line) agree well with the data for the cases of Fe and Cu targets at high velocities, and even reasonably well for a Ti target. But, for the low-Z_t targets (i.e. K and Cl), the LPA clearly under-estimates the data, even for high velocities. (The dash–double-dotted curve in the figure includes the K–K transfer contributions—for H-like and bare ions—along with the LPA predictions for ionization. The inclusion of the K–K transfer contribution improves the overall agreement with the data.) A maximum deviation of about 20–45% is to be noticed for the lowest-Z_t target that was used (i.e. for Cl), for which the asymmetry parameter ($S_Z = Z_p/Z_t$) is 0.35. It may thus be predicted that the LPA works better for more asymmetric collision partners such that $S_Z \leqslant 0.35$, above which it starts deviating.

This limitation observed here was not found in previous applications of the LPA—such as in stopping-power calculations of O ions with $v_p = 33$ au in C targets or the mixing of $n = 3$ states in Kr^{35+} with $v_p = 36$ au in Cu targets [33]—since these were studied at very high velocities. In the case of stopping power, energy straggling and K-ionization studies, the LPA model again provides good agreement for protons on Al, Si and Cu targets (see figures 1–4 in [34] and the references therein for these experimental details). Such agreement manifests the validity of the model for highly asymmetric collision systems ($S_Z \sim$ being $\frac{1}{13}$ for Al or $\frac{1}{29}$ for Cu). In all these calculations the whole set of bound electrons is taken into account instead of a single shell. This difference is important, because the FEG description given by the LPA works better when the weakly bound electrons of the more populated L or M shells are also considered [34, 37]. Very recent studies of K ionization for more symmetric collision systems at intermediate velocities, such as 1.5–6.0 MeV u^{-1} O ions on K, Cl, Ti etc, have clearly shown that the agreement with the LPA predictions was not so good. However, the agreement with the LPA model is better for the carbon data than for the oxygen data [37].

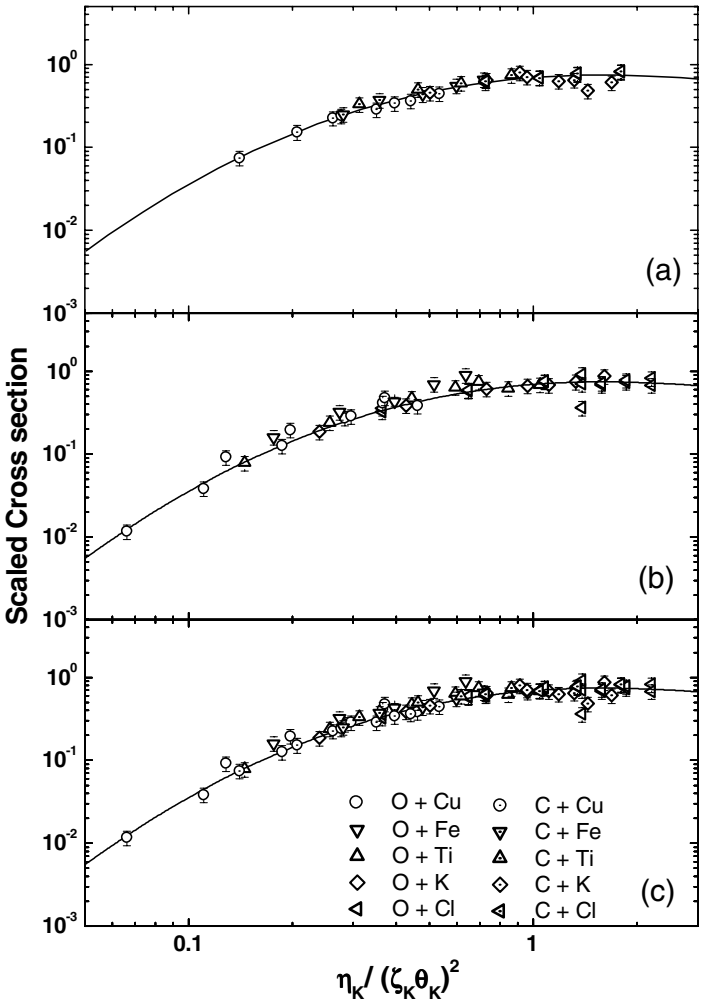

Figure 4. The universally scaled cross sections, according to the ECPSSR-predicted scaling law, as a function of scaled velocity (see text) for all the targets using (a) a C projectile, (b) an O projectile, (c) both the C and O projectiles.

The deviation of LPA calculations may be expected, since the impact velocities are mostly lower than (or approximately the same as) the electron velocity of the K shell. In these cases, the FEG approximation is supposed to fail. Two remarks must be made about the use of the LPA in K-ionization cross sections. First, the LPA calculations do not use any adjusting parameter related to the experiment, only the hard Hartree–Fock description of the target atoms. Second, a collective description of two strongly bound electrons involves using the approximation under the worst conditions. Moreover, the goal of this model is the simplicity of the description and fast calculations.

4.3.1. LPA and the generalized perturbation strength. The low-energy limit is again related to the symmetry parameter S_Z. For instance, LPA calculations for K-shell ionization of Al and Cu by proton impact reproduce the experimental data even for energies around 100 keV [34]. This relation between symmetry and impact velocities can be expressed in terms of the generalized

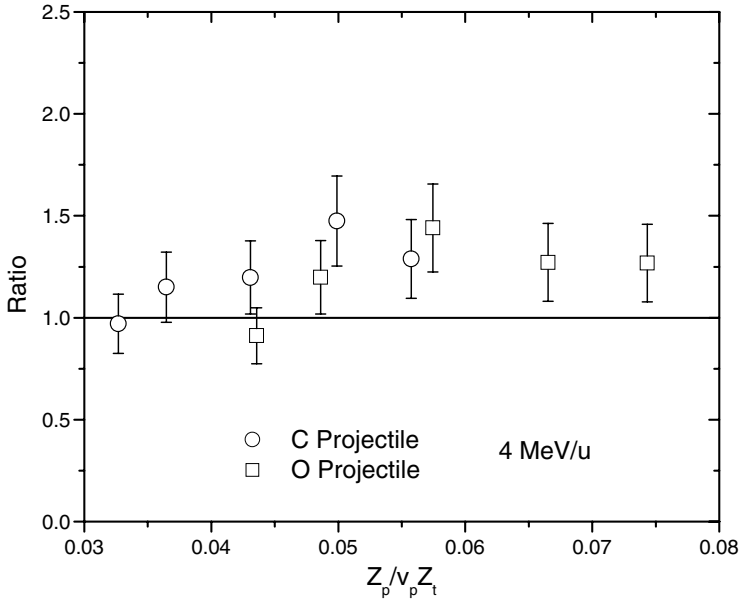

Figure 5. The ratio of the experimental cross sections to the LPA predictions as a function of generalized perturbation strength, S_p, for C and O ions [37] at 4 MeV u^{-1}.

perturbation strength $S_p = Z_p/(v_p Z_t)$ that was proposed by Tiwari *et al* [42]. To compare the deviations of the LPA predictions (σ_{KI}^{LPA}) from the experimental data (σ_{KI}^{EXP}), we plot the ratio, $\sigma_{KI}^{LPA}/\sigma_{KI}^{EXP}$, as a function of S_p at 4 MeV u^{-1} (see figure 5). The data for oxygen ions on different targets are taken from our recent work [37]. It can be clearly seen that the ratio is nearly one for the lowest value of S_p and then increases gradually with S_p, indicating increasing deviation from the LPA model. The experiment with the carbon ions enables us to extend the S_p value as low as $\sim$0.03 (at 4 MeV u^{-1}). The maximum S_p value ($\sim$0.075) was achieved using the oxygen ions. It may be concluded from both sets of data that the agreement with the LPA model is good for $S_p \leqslant 0.05$.

Although the LPA provides an acceptable result, it is not possible to make any definitive statement about the degree of solid-state effect influencing the K-ionization, since the applicability of this model is questionable in the intermediate-velocity range. However, good agreement with the ion–atom model (ECPSSR) may indicate that the influence, for the present collision systems, is negligibly small. This observation is consistent with our earlier investigations on radiative electron capture in ion–solid collisions using carbon ions with similar energies [25, 26]. It was shown that, for the case of heavy ions channelled in a Si single crystal, the radiative electron capture (REC) x-ray cross sections as well as the photon energies were about the same as those found in collisions with gaseous targets [45] for $Z_p \leqslant 9$. The comparison with the LPA proves that this ion–solid model—which includes both binary and collective mechanisms, if any [31, 35]—correctly describes typical atomic processes such as ionization of the K-shell electrons, at least for asymmetric collisions. This is also consistent with the good results found by employing the LPA for the K ionization of gases [47].

5. Conclusions

K-shell vacancy production cross sections that arise from Coulomb ionization processes in collisions with highly charged carbon ions are measured for low-atomic-number solid targets

(Z_t ranging from 17 to 29) in the intermediate-velocity range. A wide range of collision symmetry parameters (between 0.21 and 0.35) was covered. We find that all the data points follow the universal curve that was predicted by the ECPSSR formulation. The present measurements with the well known ECPSSR model show excellent agreement over the whole energy range and for all the targets considered. The good agreement of the ECPSSR clearly indicates that, for K-shell ionization, this ion–atom model is applicable for describing ion–solid collision experiments, at least for the present collision systems.

The measured ionization cross sections are used to provide a test of the LPA, based on the dielectric formalism. The LPA gives satisfactory results for the more asymmetric collisions, such as C on Ti, Fe and Cu. For lower-Z_t targets it under-estimates the data to some extent. The range of validity of the LPA, in relation to the symmetry of the collision partners, is analysed by comparing the present carbon data and recent oxygen ion data with the LPA model in terms of a generalized perturbation strength, S_p. It is shown that the LPA works better for $S_p \leqslant 0.05$.

The LPA provides acceptable overall agreement with the experimental data for K-shell ionization, with the addition of being an *ab initio* calculation which includes a detailed description of the atoms within a solid formalism. Further investigations regarding the validity of the model for inner-shell ionization must be continued. A future extension of the present work is to test LPA for L- or M-shell ionization, where the FEG description of more electrons that are less well bound is better than for the two K-shell electrons. There is still scope to improve the high-velocity model in order to explain the data in the intermediate-energy range.

Acknowledgment

The authors thank the Pelletron accelerator staff for their smooth operation of the machine.

References

[1] Stolterfoht N *et al* 1987 *Europhys. Lett.* **4** 899
[2] Fainstein P D, Ponce V H and Rivarola R D 1991 *J. Phys. B: At. Mol. Opt. Phys.* **24** 3091 and references therein
[3] Pedersen J O P, Hvelplund P, Petersen A and Fainstein P 1991 *J. Phys. B: At. Mol. Opt. Phys.* **24** 4001
[4] Stolterfoht N, Platten H, Schiwietz G, Schneider D, Gulyás L, Fainstein P D and Salin A 1995 *Phys. Rev.* A **52** 3796
[5] Tribedi L C, Richard P, Wang Y D, Lin C D, Gulyás L and Rudd M E 1998 *Phys. Rev.* A **31** 3619
[6] Tribedi L C, Richard P, DeHaven W, Gulyás L, Gealy M W and Rudd M E 1998 *J. Phys. B: At. Mol. Opt. Phys.* **31** L369
[7] Bates D R and Griffing G 1953 *Proc. Phys. Soc.* A **66** 961
[8] Crothers D S F and McCann J F 1983 *J. Phys. B: At. Mol. Phys.* **16** 3229
[9] Tribedi L C, Richard P, Gulýas L, Rudd M E and Moshammer R 2001 *Phys. Rev.* A **63** 062723
[10] Tribedi L C, Richard P, Gulýas L and Rudd M E 2001 *Phys. Rev.* A **63** 062724
[11] Dhal B B, Tribedi L C, Tiwari U, Thulasiram K V, Tandon P N, Lee T G, Lin C D and Gulýas L 2000 *Phys. Rev.* A **62** 022714
[12] Dhal B B, Tribedi L C, Tiwari U and Tandon P N 2000 *J. Phys. B: At. Mol. Opt. Phys.* **33** 1069
[13] Brandt W and Lapicki G 1981 *Phys. Rev.* A **23** 1717 and references therein
Basbas G, Brandt W and Laubert R 1973 *Phys. Rev.* A **7** 983
Basbas G, Brandt W and Laubert R 1978 *Phys. Rev.* A **17** 1655
[14] Lapicki G 1989 *J. Phys. Chem. Ref. Data* **18** 111
[15] Gray T J 1980 *Methods of Experimental Physics* vol 17, ed P Richard (New York: Academic) p 193
[16] Paul H and Muhr J 1986 *Phys. Rep.* **135** 47
[17] Braziewicz E, Braziewicz J, Pajek M, Czyzewski T, Glowacka L and Kretschmer W 1991 *J. Phys. B: At. Mol. Opt. Phys.* **24** 1669
[18] Orlic I, Sow C H and Tang S M 1994 *At. Data Nucl. Data Tables* **56** 159
[19] Hall J *et al* 1986 *Phys. Rev.* A **33** 914
[20] Tribedi L C, Prasad K G, Tandon P N, Chen Z and Lin C D 1994 *Phys. Rev.* A **49** 1015
Tribedi L C, Prasad K G and Tandon P N 1993 *Phys. Rev.* A **47** 3739

[21] Watson R L, Blackadar J M and Horvat V 1999 *Phys. Rev.* A **60** 2959
[22] Watson R L, Horvat V, Blackadar J M and Zahara K E 2000 *Phys. Rev.* A **62** 052709
[23] Dhal B B, Saha A K, Tribedi L C, Prasad K G and Tandon P N 1998 *J. Phys. B: At. Mol. Opt. Phys.* **31** L807
[24] Burgdoerfer J 1992 *Nucl. Instrum. Methods Phys. Res.* B **67** 1 and references therein
[25] Tribedi L C, Nanal V, Press M R, Kurup M B, Prasad K G and Tandon P N 1994 *Phys. Rev.* A **49** 374
[26] Tribedi L C, Nanal V, Kurup M B, Prasad K G and Tandon P N 1995 *Phys. Rev.* A **51** 1312
[27] Rozet J P, Chetioui A, Bouisset P, Vernhet D, Wohrer K, Touati A, Stephan C and Grandin J P 1987 *Phys. Rev. Lett.* **58** 337
[28] Kadhane U, Misra D, Singh Y P and Tribedi L C 2003 *Phys. Rev. Lett.* **90** 093401
[29] Kadhane U, Singh Y P, Misra D and Tribedi L C 2003 *Nucl. Instrum. Methods Phys. Res.* B **205** 661
[30] Rozet J-P, Vernhet D, Bailly-Despiney I, Fourment C and Dubé L J 1999 *J. Phys. B: At. Mol. Opt. Phys.* **32** 4677
[31] Montanari C C, Miraglia J E and Arista N R 2000 *Phys. Rev.* A **62** 052902
[32] Vernhet D, Rozet J-P, Bailly-Despiney I, Stephan C, Casssimi A, Gradin J-P and Dubé L J 1998 *J. Phys. B: At. Mol. Opt. Phys.* **31** 117
[33] Fuhr J D, Ponce V H, Garcia de Abajo P J and Echenique P M 1998 *Phys. Rev.* B **57** 9329
[34] Montanari C C, Miraglia J E and Arista N R 2002 *Phys. Rev.* A **66** 042902
[35] Arbo D G and Miraglia J E 1998 *Phys. Rev.* A **58** 2970
[36] Lindhard J 1954 *K. Dan. Vidensk. Selsk. Mat. Fys. Medd.* **28** 8
[37] Kadhane U, Montanari C C and Tribedi L C 2003 *Phys. Rev.* A **67** 032703
[38] Lindhard J and Scharff M 1953 *K. Dan. Vidensk. Selsk. Mat. Fys. Medd.* **27** 15
[39] Calera-Rubio J, Gras-Marti A and Arista N R 1994 *Nucl. Instrum. Methods Phys. Res.* B **93** 137
[40] Krause M O 1979 *J. Phys. Chem. Ref. Data* **8** 307
[41] Bhalla C P 1973 *Phys. Rev.* A **8** 2877
Bhalla C P 1975 *Phys. Rev.* A **12** 122
Bhalla C P 1975 *J. Phys. B: At. Mol. Phys.* **8** 1200
[42] Tiwari U, Saha A K, Tribedi L C, Kurup M B, Tandon P N and Gulyaś L 1998 *Phys. Rev.* A **58** 4494
[43] Lapicki G and McDaniel F D 1980 *Phys. Rev.* A **22** 1896
[44] Lapicki G and Losonsky W 1977 *Phys. Rev.* A **15** 896
[45] Vane C R, Datz S, Dittner P F, Giese J, Jones N L, Krause H F, Rosseel T M and Peterson R S 1994 *Phys. Rev.* A **49** 1847
[46] Mitra D, Singh Y P, Tribedi L C, Tandon P N and Trautmann D 2001 *Phys. Rev.* A **64** 012718
[47] Montanari C C, Miraglia J E and Arista N R 2003 *Phys. Rev.* A **67** 062702